Powerful terahertz emission from laser wakefields in inhomogeneous magnetized plasmas

Hui-Chun Wu,[1] Zheng-Ming Sheng,[1,*] Quan-Li Dong,[1] Han Xu,[2] and Jie Zhang[1]
[1]*Beijing National Laboratory for Condensed Matters, Institute of Physics, Chinese Academy of Science, Beijing 100080, China*
[2]*Institute of Computer Science, National University of Defence Technology, Changsha 410073, China*
(Received 26 April 2006; revised manuscript received 18 October 2006; published 24 January 2007)

Powerful coherent terahertz (THz) pulses with a broad spectrum (0.1–3 THz) can be produced from a laser-driven wakefield through linear mode conversion in inhomogeneous magnetized plasmas with the maximum plasma density of 10^{17} cm^{-3}. This occurs when a laser pulse, with an optimized duration about 300 fs, is incident either normally or obliquely to the density gradient of inhomogeneous magnetized plasmas. The external dc magnetic field has a magnitude of a few tesla. By changing the strength and direction of the magnetic field, one can enhance or suppress the THz emission. The maximum energy conversion efficiency in the magnetized plasmas can be double that in the unmagnetized plasmas. Such wakefield emission can be a powerful THz source at the MW level and capable of affording field strength of a few MV/cm, suitable for THz nonlinear physics. Because these THz emissions are always with a positive chirp, with a proper dispersion compression, single-cycle THz pulses can be generated with higher peak powers and field strengths.

DOI: 10.1103/PhysRevE.75.016407 PACS number(s): 52.25.Os, 52.59.Ye, 52.35.Mw

I. INTRODUCTION

Recently there has been great interest in developing high-power and -efficiency terahertz (THz) sources for applications in material characterization, imaging, and tomography [1]. Due to the low damage limit and conversion efficiency, it is difficult to obtain powerful THz emission with laser-based THz emitters, such as electro-optic crystals, semiconductors, etc. THz emission also can be produced from plasma- and electron-beam-based THz emitters, such as coherent radiation from plasma oscillations driven by ultrashort laser pulses [2], transition radiation of electron beams [3], synchrotron radiation from accelerator electrons [4], Cherenkov wake radiation in magnetized plasmas [5], and emission from laser plasma channels in air [6]. Some of these schemes can produce high-peak and/or high-average-power THz emission, though their conversion efficiencies remain low.

In Refs. [7,8], Sheng *et al.* have proposed that high-efficiency THz emissions can be produced from a laser-driven wakefield in an inhomogeneous plasma through linear mode conversion. This scheme can lead to a table-top THz source with the electric field strength over MV/cm and the power beyond megawatts. These powerful THz rays could be used for the study of new nonlinear phenomena in the THz frequency domain and in applications in high-field science. Moreover, this mechanism provides an interpretation for the early experiments [2] and theory [9], and a new diagnostic of laser wakefield amplitudes in the context of wakefield accelerators [10].

In this paper, we study the THz radiation from the laser-driven wakefield in an inhomogeneous magnetized plasma. The uniform magnetic field is perpendicular to the density gradient direction of the inhomogeneous plasma. As in the unmagnetized case [7], THz emission is produced through linear mode conversion from the electrostatic wave into electromagnetic waves. This is the inverse process of resonance absorption in laser-plasma interactions. In a magnetized plasma, it is named the upper-hybrid resonance absorption [11,12]. In the unmagnetized case, there is THz emission only when the laser light is incident obliquely to the density gradient of inhomogeneous plasmas. However, when the plasma is magnetized, there is emission for both normal and oblique incidence of the laser pulses. By changing the strength and direction of the applied magnetic field, one can enhance or suppress the THz emission. One-dimensional (1D) particle-in-cell (PIC) simulations show that THz emission with a broad spectrum (0.1–3 THz) can be produced from inhomogeneous magnetized plasmas with the maximum plasma density of 10^{17} cm^{-3}. The required dc magnetic field is a few tesla, lasting for a time scale of tens of picoseconds, which is currently available in many laboratories. The maximum conversion efficiency of the THz emission in the magnetized plasmas can be double that in the unmagnetized case.

II. CONDITION FOR LINEAR MODE CONVERSION

Let us consider the laser wakefield excitation when a plane laser pulse propagates at an angle θ to the density gradient of an inhomogeneous plasma slab in the xy plane as shown in Fig. 1. The plasma is underdense and the density rises linearly first up to $x=L$ at which the electron density is n_0, and then stays constant up to the plasma-vacuum boundary at $x=L+H$. Here, the plasma-vacuum boundary has no influence on the mode conversion. This linear density profile can be generated by a gas jet in experiments, where the peak density n_0 can be controlled to generate the wakefield at a suitable oscillation frequency. The exterior dc magnetic field $B_0\mathbf{e}_z$ is along the z direction.

Following Ref. [13], one transforms from the laboratory frame to a moving frame with the velocity $c\sin(\theta)\mathbf{e}_y$, where $\mathbf{e}_y$ is a unit vector along the y direction. We obtain (in SI units)

$$\left(\frac{\partial^2}{\partial x^2}-\frac{\partial^2}{\partial t^2}\right)\mathbf{a}=\frac{n_0}{n_c}\left[\frac{n}{\gamma\cos\theta}(a_z\mathbf{e}_z+p_y\mathbf{e}_y)+\Theta(x)\tan\theta\mathbf{e}_y\right], \quad (1)$$

*Email address: zmsheng@aphy.iphy.ac.cn

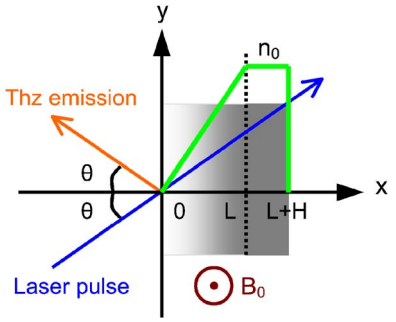

FIG. 1. (Color online) Schematic of THz emission from a wakefield excited by a laser pulse incident on an inhomogeneous magnetized plasma.

$$\frac{d}{dt}(p_y - a_y) = v_x B_0^M, \tag{2}$$

$$\frac{dp_x}{dt} = \frac{\partial \phi}{\partial x} - \mathbf{v}_\perp \cdot \frac{\partial \mathbf{a}_L}{\partial x} - E_0^M - v_y B_0^M, \tag{3}$$

$$\partial^2 \phi / \partial x^2 = (n_0/n_c)[n - \Theta(x)]/\cos\,\theta, \tag{4}$$

$$\partial n/\partial t + \partial(n v_x)/\partial x = 0, \tag{5}$$

where the wakefield vector potential $\mathbf{a}$ and laser vector potential $\mathbf{a}_L$ are normalized by mc/e, the scalar potential ϕ of the wakefield by mc^2/e, the electron density n by $n_0/\cos\,\theta$, the electron momentum $\mathbf{p}$ by mc, the electron velocity $\mathbf{v}$ by c, and x and t by c/ω_0 and ω_0^{-1}, respectively. In addition, m is the electron mass, ω_0 is the light angular frequency, $\gamma = \sqrt{1+p_x^2+p_y^2+a_z^2}$ is the electron relativistic factor, and $n_0\Theta(x)$ represents the initial plasma density distribution. Transformed from $B_0\mathbf{e}_z$ in the laboratory frame, $\mathbf{E}_0^M = B_0 \tan\,\theta \mathbf{e}_x$ and $\mathbf{B}_0^M = B_0/\cos\,\theta \mathbf{e}_z$ are the corresponding fields in the moving frame, and are normalized by $mc\omega_0/e$ and $m\omega_0/e$, respectively.

Equation (1) determines the occurrence of the low-frequency radiation from the wakefield. For $B_0=0$, Eq. (2) leads to $p_y = p_{y0} + a_y$, where $p_{y0} = -mc\,\tan\,\theta$ is the plasma streaming in the moving frame. Substituting p_y into Eq. (1), the deduced source term for THz emission is proportional to $\tan\,\theta$. Thus there is radiation only when the laser light is incident obliquely on the plasma. However, in magnetized plasmas, the new term $v_x B_0^M$, appearing in the right-hand side of Eq. (2), leads to a nonzero source even for normal incidence of the laser pulse. As in the unmagnetized case, THz emission is always p polarized, with the electric field in the xy plane and with an emitting angle θ. Usually we have $p_z = a_z = 0$ in Eq. (1) if it is satisfied initially.

It is necessary to find a proper plasma condition to make the electrostatic and electromagnetic waves phase matched, and get a high conversion efficiency. As shown in Ref. [7], if the plasma density increases linearly as $n_{0e} = n_0 x/L$, the wave vector of the wakefield in the moving frame is

$$k(x,t) = [\omega_p(x)/c](3x' - t')\cos\,\theta/2x', \tag{6}$$

where $\omega_p(x) = \omega_{p0}(x/L)^{1/2}$, $x' = x/\lambda_0$, $t' = t/\tau_0$, $\omega_{p0} = (n_0 e^2/m\varepsilon_0)^{1/2}$ is the plasma frequency, and $\tau_0 = \lambda_0/c$ is one light cycle. This suggests that the wave vector becomes zero along the line $t' = 3x'$. The longitudinal and transverse waves in plasmas can couple efficiently only at $k=0$ and $\omega = \omega_p$, where their dispersion curves meet. Along this line, the mode conversion from electrostatic to electromagnetic waves occurs. The phase velocity changes its sign around the same line. Note that Eq. (6) holds for any incident angle θ; however, for $\theta=0$, there is THz emission only in magnetized plasmas.

III. PARTICLE-IN-CELL SIMULATIONS AND MODEL CALCULATION

A. One-dimensional particle-in-cell simulations

In order to deal with the oblique incidence of the laser pulse, our PIC code adopts a boost frame moving along the y direction. We take the maximum plasma density $n_0 = 0.0001 n_c$, where $n_c = m\varepsilon_0\omega^2/e^2 = 1.1\times 10^{21}\ (\mu\mathrm{m}/\lambda_0)^2\ \mathrm{cm}^{-3}$ is the critical density for a laser pulse with wavelength λ_0 in vacuum. For $\lambda_0 = 1\ \mu$m, $n_0 = 1.1\times 10^{17}\ \mathrm{cm}^{-3}$. The corresponding plasma frequency $\omega_{p0}/2\pi = 2.98$ THz, which represents the maximum frequency of the THz emissions. The plasma wavelength $\lambda_{p0} \equiv 2\pi c/\omega_{p0} = 100\lambda_0$. We take $L = 6\lambda_{p0} = 600\lambda_0$ in the $50 \le x/\lambda_0 \le 650$ region, and $H = 50\lambda_0$ in all the simulations presented as follows.

The laser pulse, which excites a wakefield, has a sine-square profile $a_L = a_0 \sin^2[\pi(x-ct)/d_L]$ for $0 \le x - ct \le d_L$. Here a_0 is related to the peak laser intensity through $I = a_0^2 \times 1.37\times 10^{18}\ (\mu\mathrm{m}/\lambda_0)^2\ \mathrm{W/cm}^2$. We take $a_0 = 0.5$ and $d_L = 2\lambda_{p0} = 200\lambda_0$. For $\lambda_0 = 1\ \mu$m, the laser intensity $I = 3.4\times 10^{17}\ \mathrm{W/cm}^2$. The pulse enters the left boundary of the simulation box with s polarization in order to distinguish it easily from the p-polarized THz emission. All electric and magnetic fields in PIC simulations are normalized by $\omega_0 m_e c/e = 3.2\times 10^4\ (\mu\mathrm{m}/\lambda_0)$ MV/cm and $\omega_0 m_e/e = 1.1\times 10^4\ (\mu\mathrm{m}/\lambda_0)$ T, respectively. In the following, for simplicity in a practical discussion, we always take $\lambda_0 = 1\ \mu$m.

Figure 2 shows the longitudinal and transverse fields in the x-t plane, where the laser pulse is normally incident and the applied dc magnetic field $B_0 = 0.0007$, i.e., 7.7 T. One notes that the phase velocity changes its sign in the region of increasing electron density along the line $t' = 3x'$ in Fig. 2(a). Around this line, mode conversion occurs, and the electrostatic field energy is depleted soon after and converted into electromagnetic energy. Figure 2(b) shows the transverse field component E_y and Fig. 2(c) shows the component B_z. Through mode conversion, the THz emission propagates through the left vacuum-plasma boundary. Figure 2 clearly demonstrates that there are THz emissions for normal incidence of laser pulses in an inhomogeneous magnetized plasma. Note that there is no such emission at all if there is not a dc magnetic field applied in this case.

Figure 3 plots the longitudinal and transverse fields in the x-t plane, when the laser pulse is obliquely incident at the angle $\theta = 10°$, and the dc magnetic field $B_0 = 0.0003$ (3.3 T).

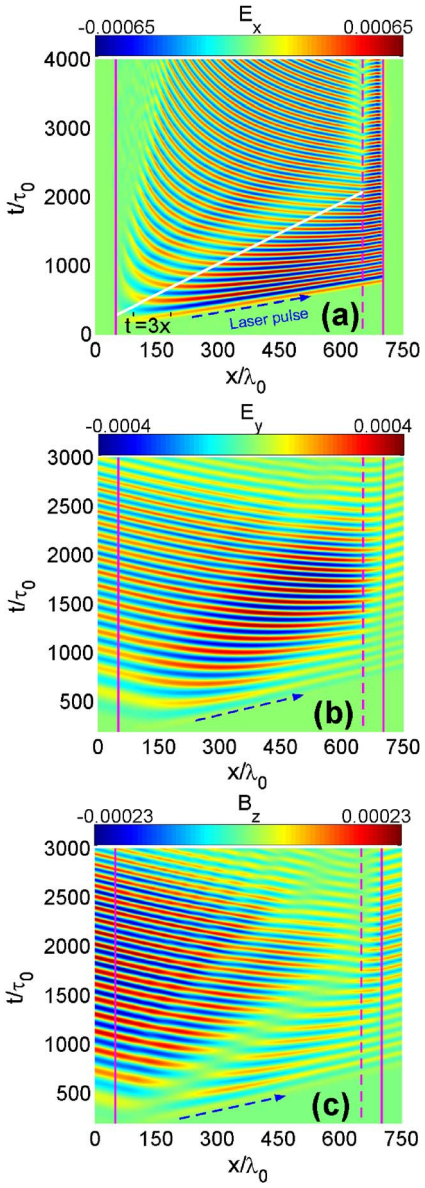

FIG. 2. (Color online) Spatial-temporal plots of the (a) longitudinal electric field E_x, (b) transverse electric field E_y, and (c) magnetic field B_z obtained from 1D PIC simulation. The laser pulse is incident normally ($\theta=0$), and has $a_0=0.5$, $d_L=200\lambda_0$. The dashed arrow points in the laser propagation direction. The external dc magnetic field is $B_0=0.0007$. The plasma has $n_0=0.0001n_c$, $L=600\lambda_0$ in the $50\leq x/\lambda_0\leq 650$ region, and $H=50\lambda_0$. The vertical solid lines represent the plasma boundaries, and the vertical dashed line is the borderline at $x/\lambda_0=650$ between the inhomogeneous and uniform regions. Mode conversion occurs around the line $t'=3x'$, displayed by the white solid line in (a).

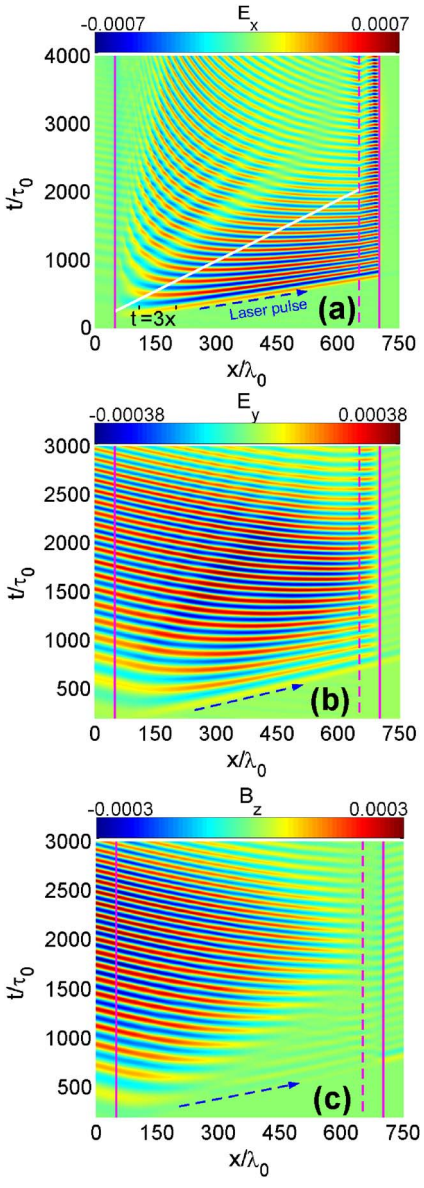

FIG. 3. (Color online) Spatial-temporal plots of the (a) longitudinal electric field E_x, (b) transverse electric field E_y, and (c) magnetic field B_z in the laboratory frame obtained from PIC simulation. The laser pulse is incident obliquely with the angle of $\theta=10°$. The external dc magnetic field is $B_0=0.0003$. Other parameters are the same as in Fig. 2.

Similar features to those shown in Fig. 2 are observed. Note that there exist phase shifts in Figs. 3(a) and 3(b). This is because, in the oblique incidence case, the electromagnetic and electrostatic components interfere with each other [7]. There is no phase quivering for the normal incidence case, because E_x in Fig. 2(a) is a purely electrostatic field, and E_y and B_z in Figs. 2(b) and 2(c) are purely electromagnetic fields. In Fig. 3(c), B_z is also a purely electromagnetic field related to the THz wave.

It is also found that there are THz emissions through the right plasma-vacuum boundaries, as shown in Figs. 2(b), 2(c), 3(b), and 3(c). This is the Cherenkov wake radiation discussed in Ref. [5]. In uniform magnetized plasmas, the wakefield itself includes both electromagnetic and electrostatic components. When the wakefield propagates through a sharp plasma-vacuum boundary, the electromagnetic component can be radiated outward. It is noted that these forward Cherenkov radiations are weaker than the backward mode-converted radiations.

B. Model calculations for normal incidence

There are two significant parameters, the incident angle θ and the magnetic field B_0, that affect the THz emission. First, we consider the effect of B_0 on the THz emission for a normally incident laser with $\theta=0$. As discussed below, the effect of B_0 on the THz spectrum and conversion efficiency is very similar to that of the incident angle θ in unmagnetized plasmas [7]. The above PIC simulations have demonstrated that there are THz emissions through linear mode conversion for a normally incident laser in a magnetized plasma. From its inverse problem, the upper-hybrid resonance absorption for normally incident laser light in a magnetized plasma [11], we have a mode conversion efficiency

$$\eta = 4\alpha \mathrm{Ai}^2(0)/\{[1+\alpha \mathrm{Ai}^2(0)]^2 + \alpha^2 \mathrm{Ai}^2(0)\mathrm{Bi}^2(0)\}, \quad (7)$$

where $\mathrm{Ai}(0)=0.355$, $\mathrm{Bi}(0)=0.615$ are constants from Airy functions. $\alpha=\pi^2(\omega_c/\omega)(L_\omega\omega/c)^{4/3}$, which depends on the external magnetic field through the electron cyclotron frequency $\omega_c=eB_0/m_e$, the local THz emission frequency ω, and the local plasma scalar length L_ω. The upper-hybrid resonance absorption occurs when $\omega=\omega_h\equiv\sqrt{\omega_p^2+\omega_c^2}$; ω_h is the upper-hybrid resonance frequency. For the linear plasma density profile $n_{0e}=n_0x/L$, $L_\omega=L(\omega_p/\omega_{p0})^2=L(\omega^2-\omega_c^2)/\omega_{p0}^2$. Defining $\tilde{\omega}=\omega/\omega_{p0}$ and $\tilde{\omega}_c=\omega_c/\omega_{p0}$, we have $\alpha=\pi^2(Lk_{p0})^{4/3}(\tilde{\omega}^2-\tilde{\omega}_c^2)^{4/3}\tilde{\omega}_c^2\tilde{\omega}^{-2/3}$, where $k_{p0}=2\pi/\lambda_{p0}\equiv\omega_{p0}/c$ is the plasma wave number. The conversion efficiency η reaches the maximum value 0.7 for $\alpha=4$.

The THz emission spectrum can be written as [7]

$$S(\tilde{\omega},\tilde{\omega}_c,L,d_L) = \eta[\alpha(\tilde{\omega},\tilde{\omega}_c,L)]E_m^2(\tilde{\omega},d_L), \quad (8)$$

where E_m is the wakefield amplitude at local frequency at the position $x=L(\tilde{\omega}^2-\tilde{\omega}_c^2)$. The wakefield amplitude in magnetized plasmas can be estimated from unmagnetized plasma theory. For a sine-square pulse $a_L=a_0\sin^2[\pi(x-ct)/d_L]$, we have the local wakefield amplitude [7,14]

$$E_m = (\tilde{\omega}\omega_{p0}m_ec/e)(a_0^2/4)\sin(\pi\tilde{\omega}\tilde{d}_L)\{[1-(\tilde{\omega}\tilde{d}_L)^2]^{-1} - 0.25[1-0.25(\tilde{\omega}\tilde{d}_L)^2]^{-1}\}, \quad (9)$$

where $\tilde{d}_L=d_L/\lambda_{p0}$.

Figure 4(a) shows the emission spectrum S for different ω_c, i.e., B_0 at fixed $L=6\lambda_{p0}$ and $d_L=2\lambda_{p0}$. For this fixed pulse duration, according to Eq. (9), the maximum wakefield amplitude appears at the frequency $\tilde{\omega}=0.75$. The maximum conversion efficiency at $\alpha=4$ leads to the optimal $\tilde{\omega}_c=0.076$. The corresponding normalized $B_0=\tilde{\omega}_c\sqrt{n_0/n_c}=0.000\,76$ (8.4 T). This is just what is shown in Fig. 4(a). At larger magnetic fields, the spectra are shifted to lower frequencies. Figure 4(b) shows the emission spectrum for different scale lengths L at the fixed $\tilde{\omega}_c=0.07$ and $d_L=2\lambda_{p0}$. It indicates that the emission depends weakly on the plasma density scale length. Figure 4(c) shows the emission spectrum as a function of the pulse duration d_L at the fixed $\tilde{\omega}_c=0.07$ and $L=6\lambda_{p0}$. It suggests that the central emission frequency is at about $\tilde{\omega}=1.5/\tilde{d}_L$, which is inversely proportional to the pulse duration d_L.

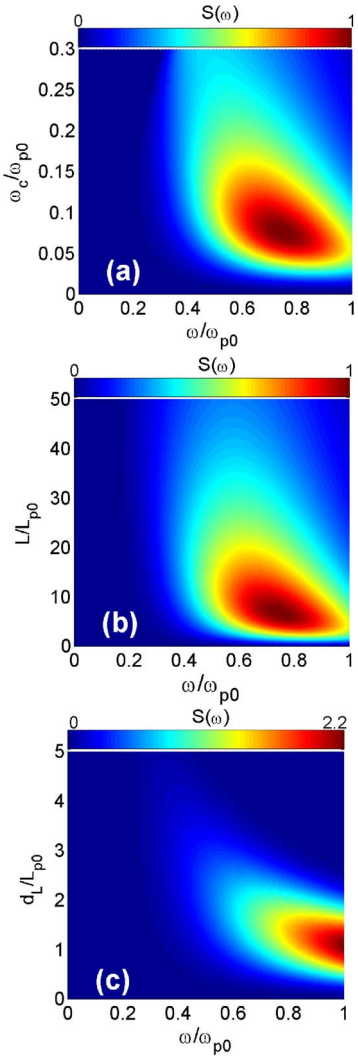

FIG. 4. (Color online) (a) Emission spectra based on Eq. (8) as a function of the electron cyclotron frequency ω_c for $L=6\lambda_{p0}$ and $d_L=2\lambda_{p0}$. (b) Emission spectra as a function of the density scale length L for $\omega_c=0.07\omega_{p0}$ and $d_L=2\lambda_{p0}$. (c) Emission spectra as a function of the pulse duration d_L for $\omega_c=0.07\omega_{p0}$ and $L=6\lambda_{p0}$. Emission spectra in (a)–(c) are in arbitrary units, but their relative amplitudes are held.

Integrating the converted energy in the inhomogeneous region divided by the laser pulse energy, we can get the energy conversion efficiency

$$\varepsilon_{\mathrm{energy}} = \frac{\int_0^L S\, d(L_\omega)}{\int_0^{d_L} E_0^2\sin^4(\pi x/d_L)dx} = \frac{4a_0^2}{3}\frac{n_0}{n_c}\frac{L}{d_L}\int_{\omega_c}^1 \eta[\alpha(\tilde{\omega},\tilde{\omega}_c,L)]\tilde{E}_m^2(\tilde{\omega},d_L)\tilde{\omega}\, d\tilde{\omega}, \quad (10)$$

where E_0 is the laser electric field, and $\tilde{E}_m$ is the wakefield amplitude normalized by $(a_0^2/2)m\omega_{p0}c/e$. We define $\varepsilon_{\mathrm{int}}$ as

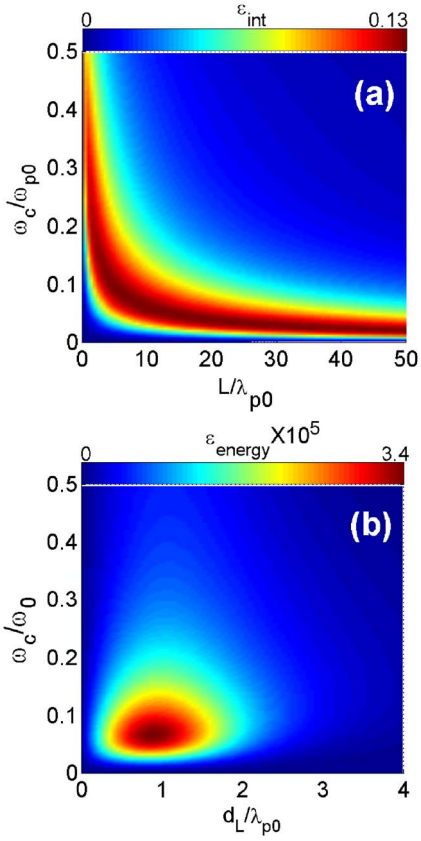

FIG. 5. (Color online) (a) The integral part ε_{int} in the $(L,\tilde{\omega}_c)$ plane for $d_L=2\lambda_{p0}$. (b) The energy conversion efficiency $\varepsilon_{\text{energy}}$ in the $(d_L,\tilde{\omega}_c)$ plane for $a_0=0.5$, $n_0=0.0001n_c$, and $L=6\lambda_{p0}$.

the integral part in Eq. (10). Because the wakefield amplitude is proportional to a_0^2, according to Eq. (10), the THz emission intensity scales like a_0^4. The energy conversion efficiency is also proportional to the plasma scale length L, since more laser energy is converted to the wakefield in a longer inhomogeneous region.

The integral factor ε_{int} depends on L, d_L, and $\tilde{\omega}_c$. Figure 5(a) shows ε_{int} in the $(L,\tilde{\omega}_c)$ plane for $d_L=2\lambda_{p0}$. ε_{int} reaches a peak value around 0.13 for a wide range of plasma density scale lengths in $\tilde{\omega}_c\in[0.03,0.1]$. Figure 5(a) also suggests that a shorter plasma scale length corresponds to a stronger magnetic field for high THz conversion efficiency. For the above simulation case with $a_0=0.5$, $n_0=0.0001n_c$, $L=6\lambda_{p0}$, $d_L=2\lambda_{p0}$, $\tilde{\omega}_c=0.07$, one obtains $\varepsilon_{\text{energy}}=1.2\times10^{-5}$.

Figure 5(b) illustrates the energy conversion efficiency $\varepsilon_{\text{energy}}$ in the $(d_L,\tilde{\omega}_c)$ plane for $a_0=0.5$, $n_0=0.0001n_c$, and $L=6\lambda_{p0}$. It is found that the optimal magnetic field is $B_0=0.000\,66$ (7.3 T), and the pulse duration is $d_L=0.82\lambda_{p0}$, for the highest conversion efficiency $\varepsilon_{\text{energy}}=3.4\times10^{-5}$.

It is interesting to note that the results in Figs. 4 and 5 are very analogous to the effects of the incident angle θ on the THz emission in unmagnetized plasmas [7], although the mode conversion mechanism is completely different.

C. Comparison between the model and simulations

To check the reliability of the above model for normal incidence, we compare the spectra predicted by the model with the simulation results. First, Fig. 6(a) shows the temporal profiles of the THz pulses for different magnetic fields B_0. The peak field strength is over 0.0002, i.e., 6.4 MV/cm. The corresponding intensity is 5.5×10^{10} W/cm^2. For a focus spot size of 150 μm ($>\lambda_{p0}$, to be discussed in Sec. IV), the corresponding peak power is about 9.7 MW and energy about 64 μJ (the THz pulse duration is about 6.6 ps). When $B_0=0.0007$, the conversion efficiency of the THz emission is 0.46×10^{-5}, which is lower than that from the model calculation given above. The reason for the model overestimate is discussed as follows.

The spectrum of the THz pulses in Fig. 6(a) is compared with that of the model calculations in Fig. 6(b). The frequency range of the THz emission is 0.1–3 THz, and it is centered at about $f_c=2$ THz. The frequency cutoff at $\omega=\omega_{p0}$ is due to the maximum electron density n_0 for the density profile in Fig. 1. It is found that, for lower magnetic field, the spectrum profiles and relative intensities agree well with each other. For higher magnetic field, the model calculation seems to overrate the spectrum intensity. This is because the local emission frequency in our model is assumed to be $\omega=\omega_h\equiv\sqrt{\omega_p^2+\omega_c^2}$. However, in practice, the frequency of the laser-driven wakefield in a magnetized plasma [15] is close to $\omega_w\equiv\sqrt{\omega_p^2(1+\omega_c^2/\omega_0^2)}$, not exactly the upper-hybrid resonance frequency ω_h. Figure 6(c) shows that the difference between ω_h and ω_w increases with the increase of B_0. This difference degrades the linear mode conversion and makes the model calculations overrate spectrum intensities and conversion efficiencies, especially for the larger magnetic field B_0.

The simulations also find that, for $a_0\leq1$, the conversion efficiency of the THz emission is proportional to a_0^4, i.e., the square of the light intensity. This agrees with the prediction of Eq. (10).

Because the emitted THz pulses are always with a positive frequency chirp as shown in Fig. 6(a), through a negative dispersion compression, one can obtain few-cycle THz pulses at higher power. We simply analyze the compression limit of these chirped pulses. For a transform-limited (chirp-free) pulse $\exp(-t^2/T^2)$, its power spectrum is proportional to $\exp(-2f^2/F^2)$; here $F=1/\pi T$. Fitting the spectra in Fig. 6(b), we get $F\approx1.2$ THz. Theoretically, the compressed pulse has a minimum duration $T=1/\pi F=0.26$ ps, which is even shorter than the oscillating cycle of the central frequency $\tau_c=1/f_c=0.5$ ps. This implies that, through a proper dispersion compression, single-cycle THz pulses with higher peak power and field strength can be produced from mode-converted emissions.

D. THz emissions for oblique incidence

Here we discuss the THz emission for oblique incidence in the magnetized plasma. Unfortunately, there is not a conversion efficiency formula like Eq. (7) in this case. Woo *et al.* [12] numerically calculated η for oblique incidence in a magnetized plasma. It is found that η is increased (decreased) when the external B_0 has the same (opposite) sign as the incident angle θ, in the interaction geometry shown in Fig. 1. The maximum value of η approaches 0.99

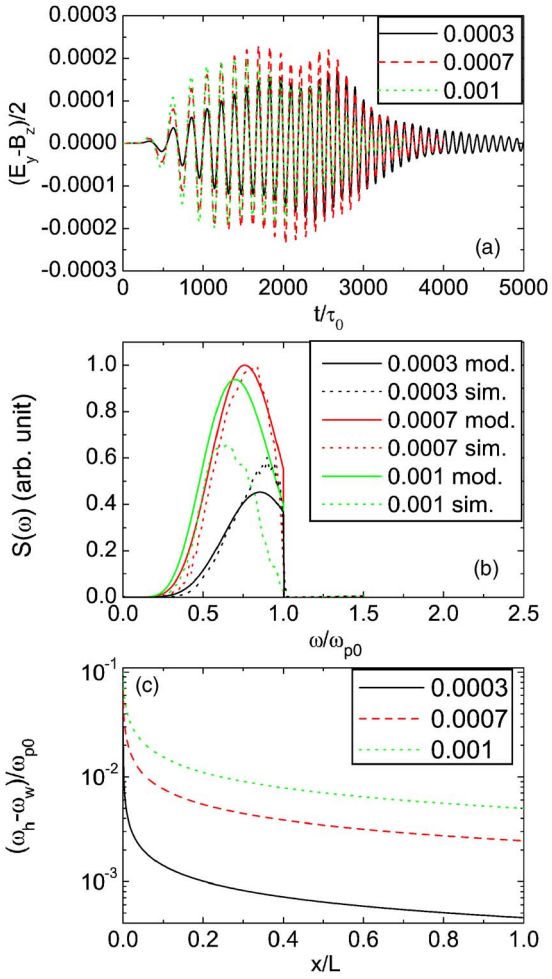

FIG. 6. (Color online) (a) Temporal profiles of the THz emissions, where $(E_y - B_z)/2$ represents the backward-propagating electromagnetic field. (b) Comparison of emission spectra between the model calculation and PIC simulations. In (a),(b), the laser pulse is normally incident ($\theta=0$). Other parameters are the same as in Fig. 2. (c) $\omega_h - \omega_w$ in the whole inhomogeneous plasma region. The numerical labels in (a)–(c) indicate the normalized magnetic fields B_0.

at the optimal $B_{0,\mathrm{opt}}$ and θ_{opt}. $\eta=0$ at $B_0=-B_{0,\mathrm{opt}}$ and $\theta=\theta_{\mathrm{opt}}$. $B_{0,\mathrm{opt}}$ is about half of the optimal B_0 for the normal incidence case. Therefore, for obliquely incident light, one can obtain higher conversion efficiencies at lower external magnetic fields.

Figure 7(a) shows the THz pulse for $B_0=0.0003$ and $\theta=10°$, the field amplitude of which is stronger than that of the optimally normal incidence case for $B_0=0.0007$ shown in Fig. 6(a). The conversion efficiency of the THz emissions is displayed in Fig. 7(b). $\theta=15°$ is the optimal incident angle for $L=6\lambda_{p0}$, $d_L=2\lambda_{p0}$ in unmagnetized plasmas [7]. One finds that the normal incidence case with $B_0=0.0007$ gives a conversion efficiency slightly higher than the unmagnetized case. This is because $\eta_{\max}=0.5$ in the unmagnetized plasma case, which is lower than $\eta_{\max}=0.7$ for normal incidence in the magnetized plasma. Moreover, the conversion efficiency at $B_0=0.0003$ and $\theta=10°$ is 1.8 times larger than in the unmagnetized case, because in this case one has $\eta_{\max}\approx 0.9$. For $B_0=-0.0003$ and $\theta=10°$ (which is equivalent to the case with

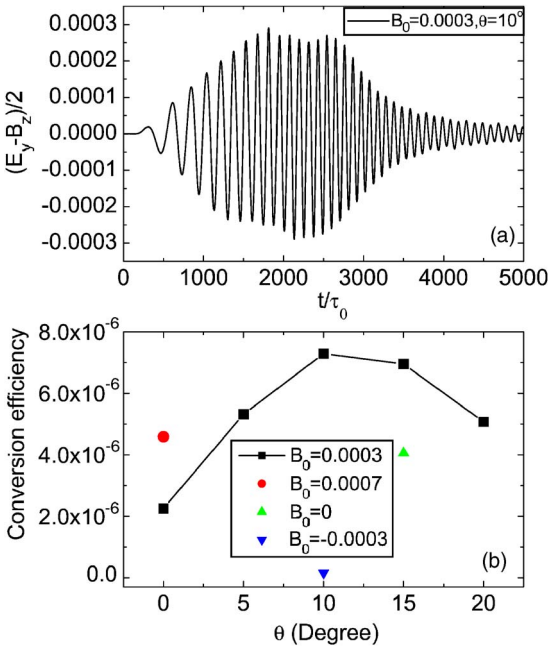

FIG. 7. (Color online) (a) Temporal profile of the THz emission. The laser pulse has the incident angle of $\theta=10°$, and the external dc magnetic field is $B_0=0.0003$. Other parameters are the same as in Fig. 3. (b) The energy conversion efficiencies of the THz emissions as a function of the incident angle θ for the magnetized and unmagnetized plasmas.

$B_0=0.0003$ and $\theta=-10°$), the THz emission is completely suppressed, as pointed out above.

IV. EFFECTS OF FINITE BEAM DIAMETER

It should be pointed out that the above 1D model calculation and 1D PIC simulations are valid as long as the laser spot size is large as compared with the plasma wavelength [8]. For a laser beam with a Gaussian profile $\exp(-r^2/w_L^2)$ in transverse space, the 1D model applies for $w_L \gg \lambda_p$. It is easily understood that, for $w_L < \lambda_p$, the radiation source size is smaller than the radiated wavelength, so that the generated THz wave will diffract dramatically. In order to obtain collimated THz emission, $w_L \gg \lambda_p$ should be maintained.

According to the angular spectrum theory, a laser beam with a finite diameter is equivalent to synthesis of many plane waves with different propagation directions. Therefore, even for a normally incident laser beam, there are obliquely incident light components. The excited plasma wave will have transverse wave vectors. One may denote its Fourier components as $W(\theta)$, which is a function of the angular direction θ. As shown in Refs. [8,9], the whole THz beam has a symmetric double-lobe shape corresponding to conical emission and is radially polarized. THz emission vanishes along the beam axis, since there is no THz emission for a normally incident plane wave in the unmagnetized plasma.

In the magnetized plasma, the effects of finite laser beam diameters are somewhat different from the unmagnetized plasma. For simplicity, we only discuss the case with $B_{0,\mathrm{opt}}$ (i.e., $B=0.0003$ for Fig. 7) and a normally incident laser

beam. There is THz emission along the beam axis for a normally incident plane wave as shown in Fig. 7(b), in contrast to its absence in an unmagnetized plasma. For the Fourier component of the incident laser beam propagating along $\theta = \theta_{opt}$ (i.e., 10° for Fig. 7), THz emission is produced with the highest efficiency and along the direction $\theta = 180° - \theta_{opt}$. THz emission amplitude in different directions depends on the conversion efficiency $\eta(\theta)$ and the weights of the different Fourier components of the laser beam $W(\theta)$, which determinate the wakefield intensity with different transverse wave vectors. The final radiated THz beam will have a peak amplitude in the region $\theta \in [180° - \theta_{opt}, 180°]$. For the Fourier component along $\theta = -\theta_{opt}$, THz emission efficiency is zero, so THz emission vanishes along $\theta = 180° + \theta_{opt}$. For the Fourier component with $\theta \in [90°, 180° - \theta_{opt}]$, there is a weak peak of the conversion efficiency η about one order smaller than $\eta_{max} = 0.99$ [12]. Thus there will also be a small THz emission peak in the region $\theta \in [180° + \theta_{opt}, 270°]$, which is much weaker than the emission peak located within $\theta \in [180° - \theta_{opt}, 180°]$. One finds that THz emission becomes asymmetric and similar to the obliquely incidence case in an unmagnetized plasma [8].

V. CONCLUSION

In conclusion, the THz emissions (0.1–3 THz) from the laser wakefields in an inhomogeneous magnetized plasma with maximum density of 10^{17} cm^{-3} have been studied by theory and PIC simulations. The emissions can be generated when the laser pulse is incident either normally or obliquely to the plasmas with an optimized pulse duration about 100 laser cycles. The THz emission is in the opposite direction of the normally incident light or the specular reflection direction of the obliquely incident pulse. The external dc magnetic field is a few tesla. By changing the strength and direction of the magnetic field, one can enhance or suppress the THz emission.

Our theory model mainly considers the normal incidence case and is valid for $a_0 \leq 1$, or weakly relativistic laser intensities. The energy conversion efficiency from the incident laser pulse increases with the scale length of the inhomogeneous plasma and the laser intensity. The model agrees with PIC simulations for both the emission spectrum and conversion efficiency. The maximum conversion efficiency of the THz emission in magnetized plasmas can be double that in unmagnetized plasmas. The emission frequency, bandwidth, and pulse duration can be controlled by the external magnetic field, incident pulse duration, incident angle, and plasma density profile. Such wakefield emission can be a powerful THz source at the megawatt level and capable of affording field strengths of a few MV/cm, suitable for THz nonlinear physics. It also provides a diagnostic method for the wakefield amplitudes in wakefield accelerators. Because this THz emission always occurs with a positive chirp, with a proper dispersion compression, single-cycle THz pulses with higher peak power and field strength can be generated.

ACKNOWLEDGMENTS

This work was supported by the China NNSF (Grants No. 10335020, No. 10425416, No. 10390160, and No. 10576035), the National High-Tech ICF Committee in China, and the Knowledge Innovation Program, CAS.

[1] B. Ferguson and X.-C. Zhang, Nat. Mater. **1**, 26 (2002).
[2] H. Hamster, A. Sullivan, S. Gordon, W. White, and R. W. Falcone, Phys. Rev. Lett. **71**, 2725 (1993); H. Hamster, A. Sullivan, S. Gordon, and R. W. Falcone, Phys. Rev. E **49**, 671 (1994).
[3] W. P. Leemans *et al.*, Phys. Rev. Lett. **91**, 074802 (2003); C. B. Schroeder, E. Esarey, J. van Tilborg, and W. P. Leemans, Phys. Rev. E **69**, 016501 (2004).
[4] G. L. Carr, M. C. Martin, W. R. McKinney, K. Jordan, G. R. Neil, and G. P. Williams, Nature (London) **420**, 153 (2002); M. Abo-Bakr, J. Feikes, K. Holldack, P. Kuske, W. B. Peatman, U. Schade, G. Wustefeld, and H.-W. Hübers, Phys. Rev. Lett. **90**, 094801 (2003).
[5] J. Yoshii, C. H. Lai, T. Katsouleas, C. Joshi, and W. B. Mori, Phys. Rev. Lett. **79**, 4194 (1997); N. Yugami, T. Higashiguchi, H. Gao, S. Sakai, K. Takahashi, H. Ito, Y. Nishida, and T. Katsouleas, *ibid.* **89**, 065003 (2002).
[6] H. Schillinger and R. Sauerbrey, Appl. Phys. B: Lasers Opt. **68**, 753 (1999); S. Tzortzakis, G. Méchain, G. Patalano, Y.-B. André, B. Prade, M. Franco, A. Mysyrowicz, J.-M. Munier, M. Gheudin, G. Beaudin, and P. Encrenaz, Opt. Lett. **27**, 1944 (2002); P. Sprangle, J. R. Penano, B. Hafizi, and C. A. Kapetanakos, Phys. Rev. E **69**, 066415 (2004); W. Hoyer, A. Knorr, J. V. Moloney, E. M. Wright, M. Kira, and S. W. Koch, Phys. Rev. Lett. **94**, 115004 (2005); X. Xie, J. Dai, and X.-C. Zhang, *ibid.* **96**, 075005 (2006).
[7] Z.-M. Sheng, K. Mima, J. Zhang, and H. Sanuki, Phys. Rev. Lett. **94**, 095003 (2005).
[8] Z.-M. Sheng, K. Mima, and J. Zhang, Phys. Plasmas **12**, 123103 (2005).
[9] Z.-M. Sheng, H.-C. Wu, K. Li, and J. Zhang, Phys. Rev. E **69**, 025401(R) (2004).
[10] Z.-M. Sheng, J. Zheng, H.-C. Wu, J. Zhang, and K. Mima, in *Proceedings of the Joint 19th International Conference on Numerical Simulation of Plasmas and 7th Asia-Pacific Plasma Theory Conference*, Nara, Japan, 2005 [J. Plasma Phys. 72, 795 (2006)].
[11] C. Grebogi, C. S. Liu, and V. K. Tripathi, Phys. Rev. Lett. **39**, 338 (1977).
[12] W. Woo, K. Estabrook, and J. S. DeGroot, Phys. Rev. Lett. **40**, 1094 (1978).
[13] R. Lichters, J. Meyer-ter-Vehn, and A. Pukhov, Phys. Plasmas **3**, 3425 (1996).
[14] Z.-M. Sheng, Y. Sentoku, K. Mima, and K. Nishihara, Phys. Rev. E **62**, 7258 (2000).
[15] C. Ren and W. B. Mori, Phys. Plasmas **11**, 1978 (2004).